

This is the accepted manuscript made available via CHORUS. The article has been published as:

# Quantum-fluctuation-induced time-of-flight correlations of an interacting trapped Bose gas

Izabella Lovas, Balázs Dóra, Eugene Demler, and Gergely Zaránd

Phys. Rev. A **95**, 023625 — Published 24 February 2017

DOI: [10.1103/PhysRevA.95.023625](https://doi.org/10.1103/PhysRevA.95.023625)

# Quantum fluctuation induced time of flight correlations of an interacting trapped Bose gas

Izabella Lovas,<sup>1</sup> Balázs Dóra,<sup>1</sup> Eugene Demler,<sup>2</sup> and Gergely Zaránd<sup>1</sup>

<sup>1</sup>MTA-BME Exotic Quantum Phases “Momentum” Research Group

Department of Theoretical Physics, Budapest University of Technology and Economics, 1111 Budapest, Budafoki út 8, Hungary

<sup>2</sup>Physics Department, Harvard University, Cambridge, Massachusetts 02138, USA

(Dated: December 16, 2016)

We investigate numerically the momentum correlations in a two dimensional, harmonically trapped interacting Bose system at  $T = 0$  temperature, by using a particle number preserving Bogoliubov approximation. Interaction induced quantum fluctuations of the quasi-condensate lead to a large anti-correlation dip between particles of wave numbers  $\mathbf{k}$  and  $-\mathbf{k}$  for  $|\mathbf{k}| \sim 1/R_c$ , with  $R_c$  typical size of the condensate. The anti-correlation dip found is a clear fingerprint of coherent quantum fluctuations of the condensate. In contrast, for larger wave numbers,  $|\mathbf{k}| \gg 1/R_c$ , a weak positive correlation is found between particles of wave numbers  $\mathbf{k}$  and  $-\mathbf{k}$ , in accordance with the Bogoliubov result for homogeneous interacting systems.

PACS numbers: 67.85.-d, 42.50.Lc, 05.30.Jp, 67.85.Hj

## I. INTRODUCTION

As demonstrated first by Hanbury Brown and Twiss, quantum statistics are efficiently probed through detecting noise correlations. In their seminal experiments Hanbury Brown and Twiss observed positive cross-correlations in the shot noise of photons emitted by independent light sources [1]. As understood later, this photon bunching originates simply from constructive interference between indistinguishable particles, obeying Bose-Einstein statistics, and has lately been also demonstrated by interferometry of bosonic atoms [2]. An analogous phenomenon is observed for fermions, where the antisymmetry of the wave function results in an anti-bunching behavior [3]. Quantum-statistics related correlations play an important role in solids, too, where they lead to the emergence of Pauli correlation-hole [4], or can conspire with interactions to lead to the emergence of magnetism [5].

Measuring Hanbury Brown Twiss-like noise correlations in time of flight (ToF) images has also been proposed as an efficient tool for detecting correlated states in ultracold atomic systems [6]. Following this suggestion, density correlations in expanding atomic clouds have been used to demonstrate the emergence of ordered phases both in interacting bosonic and fermionic systems [7–18], proving that noise detection can also be used to reveal interaction-induced strongly correlated structures.

Trapped cold atomic systems should provide an ideal test ground to study quantum correlations in isolated bosonic and fermionic systems, and the influence of interactions on these correlations [19–24]. Time of flight experiments in reduced dimensions [25] grant direct and controlled access to the observation of the number  $\hat{n}_{\mathbf{k}}$  of particles with momentum  $\hbar\mathbf{k}$  as well as to the correlation function  $C(\mathbf{k}, \mathbf{k}') \equiv \langle \delta\hat{n}_{\mathbf{k}}\delta\hat{n}_{\mathbf{k}'} \rangle$  [26–31].

For a very long time [32–35], theoretical predictions regarding the nature of momentum space correlations

and ToF correlations in Bose-systems remained somewhat controversial. Two and three dimensional weakly interacting *homogeneous* systems are quite well-described by a Bogoliubov mean field approximation, where the ground state is found to be a squeezed state generated by the pair creation operators,  $\hat{b}_{\mathbf{k}}^\dagger\hat{b}_{-\mathbf{k}}^\dagger$ , with  $\hat{b}_{\mathbf{k}}^\dagger$  denoting the creation operator of a boson [36]. This squeezed structure would imply perfect positive correlations between particles of wave numbers  $\mathbf{k}$  and  $-\mathbf{k}$  [32]. However, in a one dimensional Luttinger liquid, both correlations and anti-correlations have been predicted [32, 35], and anti-correlations have also been predicted between particles with opposite momenta [33] in harmonically confined noninteracting Bose gases.

Very recently, experiments on one-dimensional interacting bosons — corroborated by detailed theoretical calculations — managed to clarify somewhat this controversial situation [31]: they confirmed the predictions of strong *anti-correlations* of Ref. [35] at the momentum scale corresponding to the thermal length,

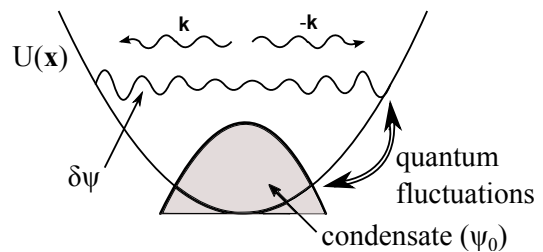


FIG. 1. Sketch of the origin of quantum fluctuations induced quasiparticle correlations in a trap. Even at  $T = 0$ , interaction-induced quantum fluctuations of the condensate induce virtual quasiparticle excitations, and amount in fluctuations and correlations, measurable through ToF experiments. The pair structure of excitations induces positive correlation between particles with opposite wave numbers  $\mathbf{k}$  and  $-\mathbf{k}$ .

$l_\phi = \rho_{1D} \hbar^2 / m k_B T$ , with  $\rho_{1D}$  the density of the one-dimensional gas.

The purpose of the present work is to understand the role of interaction-induced quantum fluctuations of higher dimensional condensates. To be specific, we focus on  $d = 2$ -dimensional interacting (quasi) condensates, where the correlation function  $C(\mathbf{k}, \mathbf{k}')$  is still directly accessible experimentally, while a mean field approach is still reliable. Extensions to  $d = 3$  dimensions are straightforward. Focusing on interaction-induced quantum fluctuations, we consider the case of  $T = 0$  temperature only [37].

In the presence of interactions, quantum fluctuations deplete the condensate wave function just as thermal fluctuations do in an ideal gas (see Fig. 1). Anti-correlations can be interpreted as a sign of conspiracy of particle number conservation and confinement: they stem from particle number preserving processes, coherently transferring particle pairs between the single mode condensate and the non-condensed fraction of the gas (see Sections III C and III D).

To capture this physics in a trapped gas, we shall employ a particle number preserving Bogoliubov approximation, similar to the one described in Ref. [38]. For sufficiently weak interactions, most of the atoms condense into a single wave function, thereby forming a single-mode condensate  $\varphi_0(\mathbf{x})$ . Correspondingly, the bosonic field operator  $\hat{\psi}(\mathbf{x})$  can be decomposed as

$$\hat{\psi}(\mathbf{x}) = \varphi_0(\mathbf{x}) \hat{b}_0 + \delta\hat{\psi}(\mathbf{x}), \quad (1)$$

where  $\hat{b}_0$  annihilates a particle from the condensate. If the average number of particles in mode  $\varphi_0(\mathbf{x})$  greatly exceeds that of non-condensed particles, the operator  $\delta\hat{\psi}(\mathbf{x})$ , describing quantum fluctuations of the condensate, is small, and can be accounted for by the particle number conserving mean field approach used here, an approach well suited to describing experiments with a fixed number of particles.

As we shall see, the spatial extension of the condensate ( $R_c$ ) takes over the role of  $l_\phi$  in one-dimensional condensates [31], and determines the region of anti-correlations in momentum space. However, in addition to anti-correlation between small momentum particles with  $\mathbf{k} \approx -\mathbf{k}'$  and  $|\mathbf{k}| \sim 1/R_c$ , a clear *forward correlation* appears for particles of similar momenta,  $\mathbf{k} \approx \mathbf{k}'$ . Momentum space correlations thus exhibit a *p-wave* structure. As already explained, these structures are due to interaction induced coherent quantum fluctuations of the condensate, present even at zero temperature.

The expected positive correlations, predicted by Bogoliubov theory, only appear at large wave numbers,  $|\mathbf{k}| \gg 1/R_c$ , where  $C(\mathbf{k}, -\mathbf{k})$  displays a slowly decaying positive tail of "*d-wave*"-like structure in momentum space. In this large momentum regime, short distance correlations at a scale  $\lambda \sim 2\pi/|\mathbf{k}|$  are probed, where correlations can be well approximated by those of a homogeneous system. The observation of Bogoliubov squeezing

and the corresponding positive pair correlations would thus require investigating the *tails* of ToF images with high resolution.

The paper is organized as follows: In Sec. II, we outline the particle number preserving Bogoliubov approximation following the treatment of Ref. [38], and provide details on the numerical solution of the corresponding equations (Sec. II B). Our results are discussed in Sec. III. Our conclusions are summarized in Sec. IV.

## II. METHODS

### A. Particle number preserving Bogoliubov approximation

We consider a closed, interacting quasi-two-dimensional Bose gas in a harmonic trap. Such quasi-two-dimensional gases can be experimentally realized in highly anisotropic harmonic potentials, where the transverse confinement,  $\omega_z$ , is much stronger than the trapping frequencies in the remaining two directions [21]. In this strong vertical confinement limit, the motion of the particles is frozen along the  $z$  direction, and the system is described by an effective  $d = 2$  dimensional Hamiltonian

$$H = \int d^2\mathbf{x} \left( \hat{\psi}^\dagger(\mathbf{x}) \left( -\frac{\hbar^2}{2m} \nabla^2 + U(\mathbf{x}) \right) \hat{\psi}(\mathbf{x}) + \frac{g}{2} \hat{\psi}^\dagger(\mathbf{x}) \hat{\psi}^\dagger(\mathbf{x}) \hat{\psi}(\mathbf{x}) \hat{\psi}(\mathbf{x}) \right). \quad (2)$$

Here  $\hat{\psi}(\mathbf{x})$  denotes the bosonic field operator, and  $m$  is the atomic mass. The harmonic potential

$$U(\mathbf{x}) = \frac{1}{2} m \omega^2 \mathbf{x}^2$$

is responsible for the weak confinement of the atoms in the lateral direction, and the interaction between the atoms is described by a repulsive Dirac-delta potential,  $V(\mathbf{x} - \mathbf{x}') = g \delta(\mathbf{x} - \mathbf{x}')$  [39]. Here the effective interaction  $g$  depends sensitively on the vertical confinement,  $\omega_z$ , and the three dimensional scattering length  $a_{3D}$  [40]. It depends, however, only logarithmically on the local chemical potential of the Bose gas, and can therefore be replaced by its value at the center of the trap for our purposes.

For sufficiently weak interactions, the majority of the atoms condenses into a single wave function, and the system can be analysed by using a Bogoliubov mean field approximation. This approach is justified if the expectation value of the number of non-condensed particles,  $\langle \delta\hat{N} \rangle$ , is only a small fraction of the total particle number  $N$ ,

$$\langle \delta\hat{N} \rangle \ll N. \quad (3)$$

This condition is necessary for a usual mean field treatment but, in  $d = 2$  dimensions, considered here, it is

not entirely equivalent to the requirement of weak interactions. A  $d = 2$  dimensional Bose gas can be considered weakly interacting even in the vicinity of the critical (Kosterlitz-Thouless) temperature  $T_c$ , provided that the dimensionless interaction strength  $\tilde{g}$  satisfies [40]

$$\tilde{g} \equiv \frac{g m}{\hbar^2} \ll 1. \quad (4)$$

Standard mean field theory can, however, be applied only in the regime where the system size is smaller than the phase correlation length. For typical weakly interacting trapped systems, the latter condition is satisfied only for temperatures  $T/T_c \lesssim 0.2$  [40, 42]. At slightly larger temperatures, but still below the critical temperature of the Kosterlitz-Thouless phase transition, a so-called quasi-condensate regime appears with large phase fluctuations. Here usual Bogoliubov mean field approach fails, however, the gradient of the phase still remains small and allows a perturbative, generalized Bogoliubov treatment [41, 42]. At  $T \approx 0$ , however, condition (4) is not necessary, and Eq. (3) is satisfied even for slightly larger interaction values,  $\tilde{g} \sim 1$ .

Below we will concentrate on the regime of true condensate, and will perform calculations at  $T = 0$  temperature. To account for correlations between the condensate and non-condensed particles, we shall use a particle number conserving Bogoliubov approach described in Ref. [38]. For that purpose, we decompose the field operator  $\hat{\psi}(\mathbf{x})$  according to Eq. (1), and separate the single mode part  $\sim \varphi_0(\mathbf{x})$ . The remaining part of the field operator,  $\delta\hat{\psi}(\mathbf{x})$ , describes interaction induced quantum fluctuations of the condensate (see Fig. 1), and can be chosen to be orthogonal to the wave function  $\varphi_0(\mathbf{x})$ ,

$$\int d^2\mathbf{x} \varphi_0^*(\mathbf{x}) \delta\hat{\psi}(\mathbf{x}) \equiv 0.$$

Next, following Refs. [38, 43], we introduce a new, particle number preserving field operator

$$\hat{\Lambda}(\mathbf{x}) \equiv \frac{1}{\hat{N}_0^{1/2}} \hat{b}_0^\dagger \delta\hat{\psi}(\mathbf{x}), \quad (5)$$

with  $\hat{N}_0 \equiv \hat{b}_0^\dagger \hat{b}_0$  denoting the number of particles condensed into the single mode part of the condensate. The field  $\hat{\Lambda}(\mathbf{x})$  satisfies the commutation relations

$$\begin{aligned} [\hat{\Lambda}(\mathbf{x}), \hat{\Lambda}(\mathbf{x}')] &= 0, \\ [\hat{\Lambda}(\mathbf{x}), \hat{\Lambda}^\dagger(\mathbf{x}')] &= \delta(\mathbf{x} - \mathbf{x}') - \varphi_0(\mathbf{x}) \varphi_0^*(\mathbf{x}') = \langle \mathbf{x} | \hat{Q}_0 | \mathbf{x}' \rangle, \end{aligned}$$

with  $\hat{Q}_0 \equiv \text{Id} - |\varphi_0\rangle\langle\varphi_0|$  denoting the projection onto the subspace orthogonal to  $|\varphi_0\rangle$ . The operator  $\hat{\Lambda}$  transfers one particle from the non-condensed fraction to the condensate, while keeping the total particle number constant. Notice that, in contrast to  $\hat{\psi}(\mathbf{x})$ ,  $\hat{\Lambda}(\mathbf{x})$  conserves the particle number, and is therefore more appropriate to describe fluctuations in a closed (microcanonical) trap.

To generate the Gross-Pitaevskii (GP) equation determining the condensate wave function  $\varphi_0(\mathbf{x})$ , we use the ansatz (1) and approximate the Hamiltonian (2) by expanding up to second order in the operator  $\hat{\Lambda} \sim \delta\hat{\psi}$ . Particle number conservation is imposed by the exact relations

$$\begin{aligned} N &= \hat{N}_0 + \delta\hat{N}, \\ \delta\hat{N} &= \int d^2\mathbf{x} \delta\hat{\psi}^\dagger(\mathbf{x}) \delta\hat{\psi}(\mathbf{x}) = \int d^2\mathbf{x} \hat{\Lambda}^\dagger(\mathbf{x}) \hat{\Lambda}(\mathbf{x}), \end{aligned}$$

which we also assert in course of the expansion. Requiring the disappearance of terms linear in  $\hat{\Lambda}$  yields the usual Gross-Pitaevskii equation for  $\varphi_0$

$$\left( -\frac{\hbar^2}{2m} \nabla^2 + U(\mathbf{x}) \right) \varphi_0(\mathbf{x}) + gN |\varphi_0(\mathbf{x})|^2 \varphi_0(\mathbf{x}) = \mu \varphi_0(\mathbf{x}), \quad (6)$$

with the Lagrange-multiplier  $\mu$  introduced to ensure that  $\varphi_0$  remain normalized. Second order terms in  $\hat{\Lambda}$  generate the equation of motion of the field operator,

$$i\partial_t \begin{pmatrix} \hat{\Lambda}(\mathbf{x}) \\ \hat{\Lambda}^\dagger(\mathbf{x}) \end{pmatrix} = \mathcal{L}_{GP}(\mathbf{x}) \begin{pmatrix} \hat{\Lambda}(\mathbf{x}) \\ \hat{\Lambda}^\dagger(\mathbf{x}) \end{pmatrix},$$

with the Bogoliubov operator  $\mathcal{L}_{GP}$  expressed as

$$\mathcal{L}_{GP} = \begin{pmatrix} Q_0 (\mathcal{H} + gN |\varphi_0|^2) Q_0 & gN Q_0 \varphi_0^2 Q_0^* \\ -gN Q_0^* (\varphi_0^*)^2 Q_0 & -Q_0^* (\mathcal{H} + gN |\varphi_0|^2) Q_0^* \end{pmatrix}, \quad (7)$$

and

$$\mathcal{H}(\mathbf{x}) = -\frac{\hbar^2}{2m} \nabla^2 + U(\mathbf{x}) - \mu + gN |\varphi_0(\mathbf{x})|^2 \quad (8)$$

denoting the mean field single particle Hamiltonian. The Lagrange-multiplier  $\mu$  appears here as a chemical potential, expressing that the condensate serves as a particle reservoir for the non-condensed fraction of the gas.

The eigenvalues and eigenvectors of the non-Hermitian operator  $\mathcal{L}_{GP}$  determine the excitation modes of the condensate. The Bogoliubov operator  $\mathcal{L}_{GP}$  has a pair of zero-modes [38, 44]

$$(\varphi_0(\mathbf{x}), 0), \quad (0, \varphi_0^*(\mathbf{x}))$$

corresponding to – physically meaningless – global phase rotations of the condensate. All other, nonzero eigenvalues of  $\mathcal{L}_{GP}$  come in pairs,  $\pm\varepsilon_s$ , and correspond to quasiparticle excitations. By denoting the eigenvector of positive eigenvalue  $\varepsilon_s > 0$  ( $s = 1, 2, \dots$ ) by  $(u_s(\mathbf{x}), v_s(\mathbf{x}))$ , we find that  $(v_s^*(\mathbf{x}), u_s^*(\mathbf{x}))$  is also an eigenvector of eigenvalue  $\varepsilon_{-s} = -\varepsilon_s$ . The positive eigenvectors of  $s, s' > 0$  satisfy the orthogonality condition

$$\int d^2\mathbf{x} (u_s^*(\mathbf{x}) u_{s'}(\mathbf{x}) - v_s^*(\mathbf{x}) v_{s'}(\mathbf{x})) = \delta_{s,s'}.$$

Moreover, together with the condensate wave function they form a complete basis, expressed by the relation

$$\sum_{\epsilon_s > 0} (u_s(\mathbf{x}) u_s^*(\mathbf{x}') - v_s^*(\mathbf{x}) v_s(\mathbf{x}')) + \varphi_0(\mathbf{x}) \varphi_0^*(\mathbf{x}') = \delta(\mathbf{x} - \mathbf{x}'). \quad (9)$$

These eigenfunctions of  $\mathcal{L}_{GP}$  can then be naturally used to expand the field operator  $\hat{\Lambda}(\mathbf{x})$  as

$$\hat{\Lambda}(\mathbf{x}) = \sum_{\epsilon_s > 0} [\hat{b}_s u_s(\mathbf{x}) + \hat{b}_s^\dagger v_s^*(\mathbf{x})], \quad (10)$$

where the  $\hat{b}_s$ 's satisfy bosonic commutation relations and annihilate quasiparticles of (positive) energy  $\epsilon_s$ . In terms of these quasiparticle excitations, within the Bogoliubov approximation, the Hamiltonian takes on a simple diagonal form

$$H = E_0 + \sum_{\epsilon_s > 0} \epsilon_s \hat{b}_s^\dagger \hat{b}_s.$$

The ground state of the system is thus simply the vacuum state of the annihilation operators  $\hat{b}_s$ . We remark that the ground state energy,  $E_0$ , incorporates interaction dependent negative corrections to the Gross-Pitaevski mean field energy, resulting from the quantum depletion of the condensate.

Let us now turn to the computation of the expectation value  $\langle \hat{n}_{\mathbf{k}} \rangle$  and the correlation function  $\langle \hat{n}_{\mathbf{k}} \hat{n}_{\mathbf{k}'} \rangle$ . The particle number operator  $\hat{n}_{\mathbf{k}}$  corresponding to wave number  $\mathbf{k}$  is defined as

$$\hat{n}_{\mathbf{k}} = \hat{\psi}_{\mathbf{k}}^\dagger \hat{\psi}_{\mathbf{k}},$$

where  $\hat{\psi}_{\mathbf{k}}$  is the Fourier-transform of the field operator,

$$\hat{\psi}_{\mathbf{k}} = \int d^2\mathbf{x} e^{-i\mathbf{k}\mathbf{x}} \hat{\psi}(\mathbf{x}).$$

In order to calculate the expectation value and correlation function of the operator  $\hat{n}_{\mathbf{k}}$ , we use Eqs. (1) and (5)

to express  $\hat{n}_{\mathbf{k}}$  in terms of the operator  $\hat{\Lambda}$ , to find

$$\hat{n}_{\mathbf{k}} = N|\varphi_0(\mathbf{k})|^2 - |\varphi_0(\mathbf{k})|^2 \delta \hat{N} + \sqrt{N} \varphi_0^*(\mathbf{k}) \hat{\Lambda}_{\mathbf{k}} + \sqrt{N} \varphi_0(\mathbf{k}) \hat{\Lambda}_{\mathbf{k}}^\dagger + \hat{\Lambda}_{\mathbf{k}}^\dagger \hat{\Lambda}_{\mathbf{k}} + \mathcal{O}(\delta \hat{N}^{3/2} N^{-1/2}), \quad (11)$$

with  $\hat{\Lambda}_{\mathbf{k}}$  denoting the Fourier transform of  $\hat{\Lambda}$ ,

$$\hat{\Lambda}_{\mathbf{k}} = \sum_{\epsilon_s > 0} [\hat{b}_s u_s(\mathbf{k}) + \hat{b}_s^\dagger v_s^*(-\mathbf{k})].$$

Notice that the second term in Eq. (11) does not appear in the usual Bogoliubov approach. It is a direct consequence of the particle number conserving method, and leads to corrections in the expressions of the correlation functions. This term may be contrasted to the third and fourth terms, which are also related to particle number conserving processes but appear already within the usual Bogoliubov approach; these describe the annihilation (creation) of a particle in the cloud of quantum fluctuations, while adding (removing) a particle to the condensate (from the condensate).

Notice that the usual and heuristic identification,  $\hat{n}_{\mathbf{k}} \leftrightarrow \hat{\Lambda}_{\mathbf{k}}^\dagger \hat{\Lambda}_{\mathbf{k}}$  is not appropriate for a trapped micro-canonical condensate, where correlations between the single mode part of the condensate and  $\delta \hat{\psi}(\mathbf{x})$  cannot be neglected. For a homogeneous condensate, however,  $\varphi_0^{\text{hom}}(\mathbf{k} \neq 0) \equiv 0$ , and Eq. (11) reduces to the simple relation,  $\hat{n}_{\mathbf{k} \neq 0}^{\text{hom}} = \hat{\Lambda}_{\mathbf{k}}^\dagger \hat{\Lambda}_{\mathbf{k}}$ .

The ground state expectation value of  $\hat{n}_{\mathbf{k}}$  is thus given in terms of eigenfunctions  $(u_s(\mathbf{x}), v_s(\mathbf{x}))$  as

$$\langle n_{\mathbf{k}} \rangle = N|\varphi_0(\mathbf{k})|^2 + \sum_{\epsilon_s > 0} |v_s(-\mathbf{k})|^2 - |\varphi_0(\mathbf{k})|^2 \sum_{\epsilon_s > 0} \int d^2\mathbf{x} |v_s(\mathbf{x})|^2. \quad (12)$$

Here the first term is simply the Gross-Pitaevskii result, describing a situation when all particles belong to the single-mode condensate. The sum  $\sum_s |v_s(-\mathbf{k})|^2$  takes into account the contribution of the non-condensed fraction of the gas, while the last term originates from the depletion of the condensate due to particle number conservation. Similarly, the correlation function of  $\hat{n}_{\mathbf{k}}$  and  $\hat{n}_{\mathbf{k}'}$  operators can be expressed as

$$\begin{aligned} C(\mathbf{k}, \mathbf{k}') &= \langle \hat{\psi}_{\mathbf{k}}^\dagger \hat{\psi}_{\mathbf{k}} \hat{\psi}_{\mathbf{k}'}^\dagger \hat{\psi}_{\mathbf{k}'} \rangle - \langle \hat{\psi}_{\mathbf{k}}^\dagger \hat{\psi}_{\mathbf{k}} \rangle \langle \hat{\psi}_{\mathbf{k}'}^\dagger \hat{\psi}_{\mathbf{k}'} \rangle = \\ &= N \sum_s (\varphi_0^*(\mathbf{k}) u_s(\mathbf{k}) + \varphi_0(\mathbf{k}) v_s(-\mathbf{k})) (\varphi_0(\mathbf{k}') u_s^*(\mathbf{k}') + \varphi_0^*(\mathbf{k}') v_s^*(-\mathbf{k}')) \\ &+ \sum_{s_1, s_2, s_3, s_4} (\delta_{s_1, s_4} \delta_{s_2, s_3} + \delta_{s_1, s_3} \delta_{s_2, s_4}) \left( v_{s_1}(-\mathbf{k}) u_{s_2}(\mathbf{k}) - |\varphi_0(\mathbf{k})|^2 \int d^2\mathbf{x} v_{s_1}(\mathbf{x}) u_{s_2}(\mathbf{x}) \right) \\ &\left( v_{s_4}^*(-\mathbf{k}') u_{s_3}^*(\mathbf{k}') - |\varphi_0(\mathbf{k}')|^2 \int d^2\mathbf{x} v_{s_4}^*(\mathbf{x}) u_{s_3}^*(\mathbf{x}) \right). \end{aligned}$$

This equation can be rewritten in a form more convenient for numerical calculations, using the completeness relation Eq. (9). Expressing  $\sum_s u_s(\mathbf{k})u_s^*(\mathbf{k}')$  from the Fourier transform of Eq. (9) allows us to separate the singular,  $\sim \delta(\mathbf{k} - \mathbf{k}')$  terms appearing in the diagonal correlation function  $C(\mathbf{k}, \mathbf{k})$ . As a result, the correlation

function can be written as a sum of three contributions

$$C(\mathbf{k}, \mathbf{k}') = (2\pi)^2 \delta(\mathbf{k} - \mathbf{k}') \langle \hat{n}_{\mathbf{k}} \rangle + C^{(1)}(\mathbf{k}, \mathbf{k}') + C^{(2)}(\mathbf{k}, \mathbf{k}'), \quad (13)$$

with  $\langle \hat{n}_{\mathbf{k}} \rangle$  given by Eq. (12), and

$$\begin{aligned} C^{(1)}(\mathbf{k}, \mathbf{k}') &\equiv N \sum_s [\varphi_0^*(\mathbf{k})\varphi_0^*(\mathbf{k}') u_s(\mathbf{k}) v_s^*(-\mathbf{k}') + \varphi_0(\mathbf{k})\varphi_0(\mathbf{k}') v_s(-\mathbf{k}) u_s^*(\mathbf{k}') + \varphi_0(\mathbf{k})\varphi_0^*(\mathbf{k}') v_s(-\mathbf{k}) v_s^*(-\mathbf{k}') \\ &\quad + \varphi_0^*(\mathbf{k})\varphi_0(\mathbf{k}') v_s^*(-\mathbf{k}) v_s(-\mathbf{k}')] - N |\varphi_0(\mathbf{k})|^2 |\varphi_0(\mathbf{k}')|^2, \\ C^{(2)}(\mathbf{k}, \mathbf{k}') &\equiv \sum_{s_1, s_2} \left( v_{s_1}(-\mathbf{k}) u_{s_2}(\mathbf{k}) - |\varphi_0(\mathbf{k})|^2 \int d^2\mathbf{x} v_{s_1}(\mathbf{x}) u_{s_2}(\mathbf{x}) \right) \left( v_{s_2}^*(-\mathbf{k}') u_{s_1}^*(\mathbf{k}') - |\varphi_0(\mathbf{k}')|^2 \int d^2\mathbf{x} v_{s_2}^*(\mathbf{x}) u_{s_1}^*(\mathbf{x}) \right) \\ &\quad + \sum_{s_1, s_2} \left( v_{s_1}(-\mathbf{k}) v_{s_2}^*(-\mathbf{k}) - |\varphi_0(\mathbf{k})|^2 \int d^2\mathbf{x} v_{s_1}(\mathbf{x}) v_{s_2}^*(\mathbf{x}) \right) \left( v_{s_1}^*(-\mathbf{k}') v_{s_2}(-\mathbf{k}') - |\varphi_0(\mathbf{k}')|^2 \int d^2\mathbf{x} v_{s_1}^*(\mathbf{x}) v_{s_2}(\mathbf{x}) \right) \\ &\quad - \varphi_0(\mathbf{k})\varphi_0^*(\mathbf{k}') \sum_s v_s(-\mathbf{k}) v_s^*(-\mathbf{k}') - |\varphi_0(\mathbf{k})|^2 \sum_s |v_s(-\mathbf{k}')|^2 - |\varphi_0(\mathbf{k}')|^2 \sum_s |v_s(-\mathbf{k})|^2 \\ &\quad + |\varphi_0(\mathbf{k})|^2 |\varphi_0(\mathbf{k}')|^2 \sum_s \int d^2\mathbf{x} |v_s(\mathbf{x})|^2. \end{aligned} \quad (14a)$$

Here, besides Eq. (9), we have used that the eigenfunctions  $u_s$  and  $v_s^*$  are orthogonal to the condensate wave function  $\varphi_0$ .

The first term in Eq. (13) denotes the shot noise. The first correction,  $C^{(1)}(\mathbf{k}, \mathbf{k}')$ , is proportional to the total particle number  $N$ , and includes terms of second order in fluctuations,  $\mathcal{O}(|\delta\psi|^2)$ , describing correlations between the single mode condensate and the non-condensed part of the wave function [45]. The second correction,  $C^{(2)}(\mathbf{k}, \mathbf{k}')$ , is of fourth order in fluctuations,  $\mathcal{O}(|\delta\psi|^4)$ , and takes into account correlations inside the non-condensed cloud and subleading corrections to the condensate - quasiparticle correlations contained in  $C^{(1)}$ . These latter are generated by the second term in Eq. (11), and account for the depletion of the single mode condensate. The "cylindrically symmetrical" terms in Eq. (14b), proportional to  $|\varphi_0(\mathbf{k})|^2$  (or  $|\varphi_0(\mathbf{k}')|^2$ ), stem from correlations between the condensate and the non-condensed fraction of the gas, and only appear in the particle number preserving Bogoliubov approach. The remaining terms in  $C^{(2)}$  describe correlations inside the non-condensed cloud.

## B. Numerical solution

To evaluate the expectation value (12) and the correlation functions (14a) and (14b), we first need to compute  $\varphi_0$  by solving the inhomogeneous Gross-Pitaevskii equations (6) numerically, and we then have to determine the spectrum of  $\mathcal{L}_{GP}$ . For this purpose, we shall expand all wave functions in terms of two dimensional harmonic os-

cillator eigenfunctions [46].

As a first step, we introduce the dimensionless variables [47]

$$\zeta = \frac{\hbar\omega}{2\mu}, \quad y_i = \frac{x_i}{R_c},$$

with  $R_c = \sqrt{2\mu/m\omega^2}$  denoting the size of the condensate, and rewrite all equations in terms of dimensionless parameters. The dimensionless condensate wave function  $\phi_0$  of  $N$  bosons can then be expressed as

$$\phi_0(\mathbf{y}) \equiv \sqrt{N} R_c \varphi_0(\mathbf{y} R_c).$$

This function is normalized to  $N$  and, by Eq. (6), minimizes the dimensionless energy functional

$$\begin{aligned} \mathcal{E}_0 &= \int d^2\mathbf{y} \left( \zeta^2 |\nabla_{\mathbf{y}} \phi_0(\mathbf{y})|^2 + (\mathbf{y}^2 - 1) |\phi_0(\mathbf{y})|^2 \right. \\ &\quad \left. + \frac{g}{2\mu R_c^2} |\phi_0(\mathbf{y})|^4 \right). \end{aligned}$$

We can therefore determine it by expanding  $\phi_0(\mathbf{y})$  in terms of  $d = 2$  dimensional harmonic oscillator eigenfunctions,

$$\phi_0(y) = \sum_{k=0}^{k_{\text{cut}}} a_k e^{-\frac{y^2}{2\zeta}} L_k \left( \frac{y^2}{\zeta} \right),$$

with  $L_k$  the  $k$ 'th Laguerre-polynomial and  $k_{\text{cut}}$  finite cut-off introduced for numerical calculations, and then by determining the coefficients  $a_k$  via the gradient method.

Having the condensate wave function  $\phi_0$  at hand, we determine the Bogoliubov eigenfunctions  $u_s(\mathbf{x})$  and  $v_s(\mathbf{x})$  by solving the eigenvalue equation of  $\mathcal{L}_{GP}$ . In order to take into account the projection  $\hat{Q}_0$  in Eq. (7), we modify  $\mathcal{L}_{GP}$  by a 'Lagrange multiplier'

$$\mathcal{L}'_{GP} = \begin{pmatrix} \mathcal{H} + gN|\varphi_0|^2 + \lambda P_0 & gN\varphi_0^2 \\ -gN(\varphi_0^*)^2 & -\mathcal{H} - gN|\varphi_0|^2 + \lambda P_0 \end{pmatrix}, \quad (15)$$

with  $\hat{P}_0 \equiv |\varphi_0\rangle\langle\varphi_0|$  denoting the projection to the condensate wave function and  $\mathcal{H}$  the mean field Hamiltonian, given by Eq. (8). The parameter  $\lambda$  is chosen to be large enough to ensure that the low energy eigenfunctions of  $\mathcal{L}'_{GP}$ , orthogonal to  $\varphi_0$ , be clearly separated from the high energy spectrum, having finite overlap with the condensate wave function. By keeping only the eigenfunctions of low eigenvalues, annihilated by  $\hat{P}_0$ , we can determine the excitation spectrum and eigenvectors of the original projected Bogoliubov operator  $\mathcal{L}_{GP}$ .

Similar to  $\phi_0$ , we determine the eigenfunctions  $u_s(\mathbf{x})$  and  $v_s(\mathbf{x})$  from the eigenvalue equation of  $\mathcal{L}'_{GP}$  by expanding them in terms of oscillator eigenfunctions. The calculation can be simplified by making use of the rotational symmetry of the condensate, and treating sectors with different angular momenta  $m$  separately. Eigenvectors can then be classified using radial and angular momentum indices,  $s = (n, m)$ , and the eigenfunctions can be expanded in polar coordinates as

$$\begin{pmatrix} u_{n,m}(\mathbf{y}) \\ v_{n,m}(\mathbf{y}) \end{pmatrix} = \sum_{k=0}^{k_{\text{cut}}} \begin{pmatrix} \alpha_{nk}^{(m)} \\ \beta_{nk}^{(m)} \end{pmatrix} e^{im\varphi} \left( \frac{y}{\sqrt{\zeta}} \right)^{|m|} L_k^{(|m|)} \left( \frac{y^2}{\zeta} \right) e^{-\frac{y^2}{2\zeta}}, \quad (16)$$

with  $L_k^{(|m|)}$  denoting the generalized Laguerre polynomial of indices  $k$  and  $|m|$ . Substituting this expression into the eigenvalue equations (15) allows us to determine the coefficients  $\alpha_{nk}^{(m)}$  and  $\beta_{nk}^{(m)}$ . Finally, as a last step, we can now take the Fourier transform of the functions  $\phi_0(\mathbf{y})$ ,  $u_s(\mathbf{y})$  and  $v_s(\mathbf{y})$  numerically and evaluate the expectation value  $\langle \hat{n}_{\mathbf{k}} \rangle$  and the correlation function  $C(\mathbf{k}, \mathbf{k}')$  [48].

### III. RESULTS

#### A. Wave functions

Typical examples of the condensate wave functions and the radial parts of the Bogoliubov eigenfunctions are shown in Fig. 2. The anomalous component of the quasiparticle wave function,  $v_{n,m}(y)$ , originates from the interaction with the single-mode part of the condensate, and its support is determined by the extension of the latter. In contrast, the normal component  $u_{n,m}(y)$  is not constrained to the regime  $\varphi_0 \neq 0$ , and for high energy

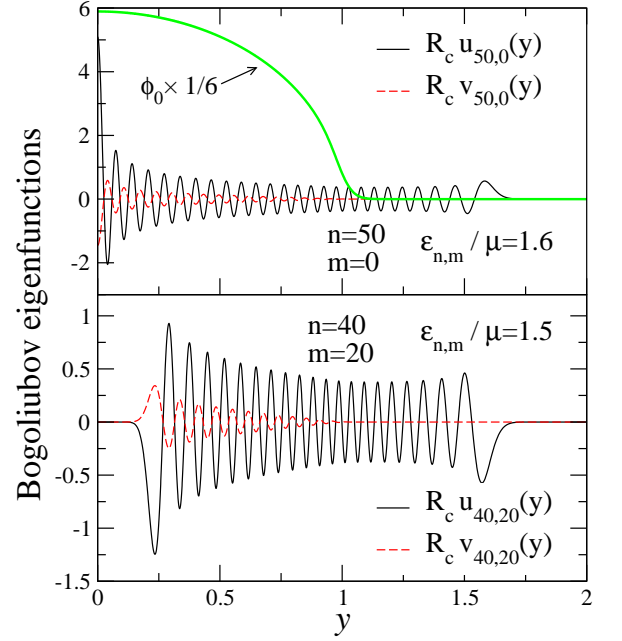


FIG. 2. Radial part of the dimensionless Bogoliubov eigenfunctions  $R_c u_{n,m}(\mathbf{x})$ ,  $R_c v_{n,m}(\mathbf{x})$  plotted as a function of the dimensionless radial coordinate  $y = |\mathbf{x}|R_c$  for  $(n, m) = (50, 0)$  (top) and  $(n, m) = (40, 20)$  (bottom), corresponding to excitation energies  $\varepsilon_{50,0}/\mu = 1.6$  and  $\varepsilon_{40,20}/\mu = 1.5$  respectively. Here  $R_c = \sqrt{2\mu/(m\omega^2)}$  is the typical size of the condensate,  $\zeta^{-1} = 2\mu/(\hbar\omega) = 100$  and  $\mu R_c^2/g = 1250$ , corresponding to  $N = 1962$  particles and  $\langle \delta \hat{N} \rangle = 608$ . In the top figure, the dimensionless single-mode condensate wave function  $\phi_0$  is also displayed. The anomalous part  $v_{n,m}$  is nonzero only in the regime of the condensate, while the normal part  $u_{n,m}$  of the wave function can be more extended. For  $m \neq 0$  both  $u_{n,m} \rightarrow 0$  and  $v_{n,m} \rightarrow 0$  at the center of the trap.

quasiparticles it resembles to a harmonic oscillator wave function. Furthermore, as the corresponding excitation energy  $\varepsilon_{n,m}$  increases, the interaction energy becomes negligible compared to the kinetic and potential energies, leading to a decrease in the amplitude of  $v_{n,m}(y)$ .

The Fourier transforms of the radial parts of the eigenfunctions are plotted as a function of the dimensionless wave number  $|\mathbf{k}|R_c$  in Fig. 3. The normal component  $u_{n,m}(k)$  involves many momenta, and is therefore quite extended in Fourier space. The Fourier transform of the anomalous component  $v_{n,m}(k)$ , however, exhibits a well-defined peak at  $\mathbf{k}_{\text{peak}}$ . This is explained by the fact that  $v_{n,m}(y)$  is constrained to the regime where the condensate is present, and there it oscillates with an approximately constant radial wave number,  $\mathbf{k} \approx \mathbf{k}_{\text{peak}}$ .

#### B. Particle number distributions

The expectation values of the particle number  $\hat{n}_{\mathbf{k}}$ , determined from Eq.(12), are plotted in Fig. 4 for different

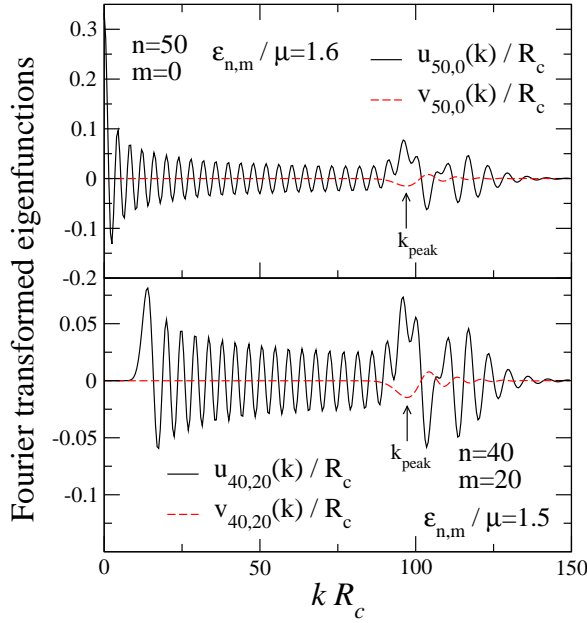


FIG. 3. Radial part of the dimensionless Fourier transformed Bogoliubov eigenfunctions  $u_{n,m}(\mathbf{k})/R_c$ ,  $v_{n,m}(\mathbf{k})/R_c$  as a function of the dimensionless wave number  $|\mathbf{k}|R_c$  for  $(n, m) = (50, 0)$  and  $(n, m) = (40, 20)$ , corresponding to excitation energies  $\varepsilon_{50,0}/\mu = 1.6$  and  $\varepsilon_{40,20}/\mu = 1.5$  respectively. Here  $R_c = \sqrt{2\mu}/(m\omega^2)$  typical size of the condensate,  $\zeta^{-1} = 2\mu/(\hbar\omega) = 100$ , and  $\mu R_c^2/g = 1250$ , corresponding to  $N = 1962$  particles and  $\langle \hat{N} \rangle = 608$ . The anomalous component  $v_{n,m}(\mathbf{k})$  has a well defined peak at wave number  $|\mathbf{k}_{\text{peak}}|$  and vanishes for lower  $|\mathbf{k}|$ , while the normal part  $u_{n,m}(\mathbf{k})$  is extended in momentum space.

dimensionless interaction strengths  $\tilde{g}$ . The contribution  $\langle \delta \hat{n}_{\mathbf{k}} \rangle$  of the non-condensed particles is shown separately. The expectation values are dominated by the single mode part of condensate, giving rise to a large and narrow peak at small wave numbers,  $|\mathbf{k}| \lesssim 1/R_c$ . Increasing  $\tilde{g}$  amounts in more extended condensate wave functions in real space, and thereby a narrower peak in  $\langle \hat{n}_{\mathbf{k}} \rangle$ . The non-condensed fraction,  $\langle \delta \hat{n}_{\mathbf{k}} \rangle$ , gives only a negligible correction for small momenta,  $|\mathbf{k}| \lesssim 1/R_c$ . However, it decays approximately as  $1/|\mathbf{k}|$ , much more slowly than the central condensate peak, and dominates the *large* wave number behavior,  $|\mathbf{k}| > 1/R_c$ . For even larger values beyond the inverse healing length,  $|\mathbf{k}| \gg \sqrt{m\mu}/\hbar \equiv \xi_h^{-1}$ ,  $\langle \delta \hat{n}_{\mathbf{k}} \rangle$  goes rapidly to zero in a universal fashion as  $\sim 1/|\mathbf{k}|^4$  [30, 49, 50] (see also Fig. 5). Although small in amplitude, the contribution from  $\delta n_{\mathbf{k}}$  hosts about  $\sim 30\%$  of the particles for the interactions considered here. Increasing  $\tilde{g}$  depletes the condensate further and leads to a gradual increase in  $\langle \delta \hat{n}_{\mathbf{k}} \rangle$ .

The expectation value of the non-condensed fraction,  $\langle \delta \hat{n}_{\mathbf{k}} \rangle$ , is investigated in more detail in Fig. 5, where we compare our numerical results with the momentum distribution of a homogeneous gas. Decreasing the trapping frequency  $\omega$ , while keeping the density of the condensate

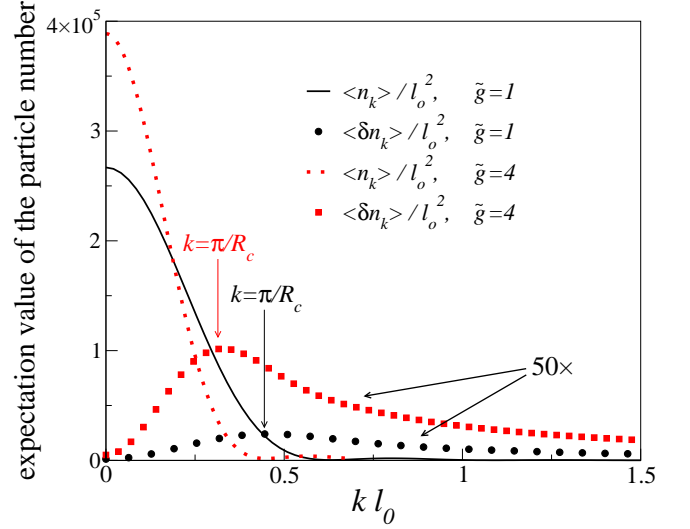


FIG. 4. Dimensionless expectation values  $\langle \hat{n}_{\mathbf{k}} \rangle / l_0^2$  as a function of  $|\mathbf{k}| l_0$  for  $N = 1962$  and for dimensionless interaction strengths  $\tilde{g} = 1$  and  $\tilde{g} = 4$ , corresponding to  $\langle \hat{N} \rangle = 145$  and  $\langle \hat{N} \rangle = 608$ . Dotted lines represent contributions of non-condensed particles  $\langle \delta \hat{n}_{\mathbf{k}} \rangle / l_0^2$ , with  $l_0 = \sqrt{\hbar}/(m\omega)$ , multiplied by a factor of 50 for better visibility. The extension of the condensate increases with increasing  $\tilde{g}$ , and the peak in  $\langle \hat{n}_{\mathbf{k}} \rangle$  gets narrower. The long tail quasiparticle contributions  $\langle \delta \hat{n}_{\mathbf{k}} \rangle$  get more pronounced with increasing  $\tilde{g}$ .

at the center of the trap and the interaction strength (or, equivalently, the healing length  $\xi_h = \hbar/\sqrt{m\mu}$ ) constant, amounts in a slowly varying condensate wave function in a wide central region. Therefore, in this limit, a homogeneous system is expected to yield a good approximation for the non-condensed fraction  $\langle \delta \hat{n}_{\mathbf{k}} \rangle$ . To make a precise comparison, however, we need to keep in mind that  $n_{\mathbf{k}}$  is dimensionful, and scales as  $n_{\mathbf{k}} \sim (\text{length})^2$ . In our case, the size of the condensate  $R_c$  plays the role of the system size  $L$  of a homogeneous system. Therefore, to recover the homogeneous result, we need to investigate the dimensionless expectation value  $\langle \delta \hat{n}_{\mathbf{k}} \rangle / R_c^2$ . Since the density of the condensate at the center of the trap scales as  $\rho(0) \sim N/R_c^2 \sim N\zeta^2/\xi_h^2$ , we calculated  $\langle \delta \hat{n}_{\mathbf{k}} \rangle / R_c^2$  for different  $\zeta$  values, while keeping  $N\zeta^2$  and  $\xi_h$  constant. As shown in Fig. 5, with decreasing  $\omega$ , the height of the peak in  $\langle \delta \hat{n}_{\mathbf{k}} \rangle / R_c^2$  scales as  $\sim 1/\omega$ , and the peak position shifts to smaller wave numbers, such that the high momentum part traces out a common envelope function, just the momentum distribution of a homogeneous gas.

The momentum distribution of a homogeneous system of size  $R_c$  and density  $\rho_0$  is given by [51]

$$\frac{\langle \delta \hat{n}_{\mathbf{k}} \rangle_{\text{hom}}}{R_c^2 \pi} = \frac{1}{2} \left( \frac{(k\xi_h^0)^2 + 2}{\sqrt{(k\xi_h^0)^2((k\xi_h^0)^2 + 4)}} - 1 \right), \quad (17)$$

with  $\xi_h^0 = \hbar/\sqrt{mg\rho_0}$  the healing length of the homogeneous gas, and  $R_c^2 \pi$  the volume of the cylindrically



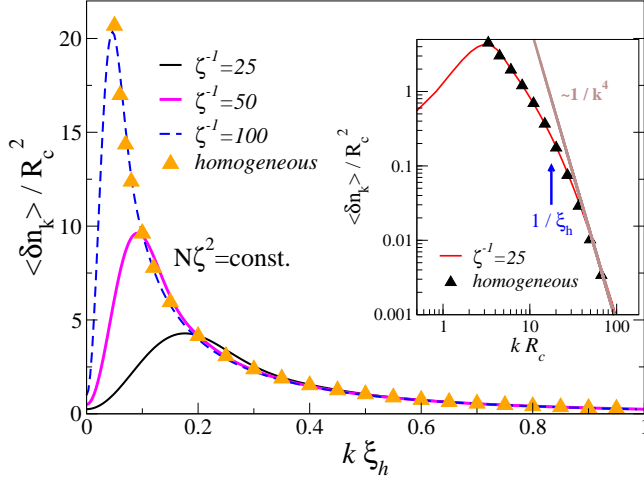


FIG. 5. Scaling collapse of  $\langle \delta \hat{n}_{\mathbf{k}} \rangle^2 / R_c^2$ , plotted as a function of  $k \xi_h$  for different  $\zeta = \hbar\omega/(2\mu)$ 's, while keeping  $\tilde{g} = 4$  and  $\rho(0)$  constant. Here  $R_c = \sqrt{2\mu/(m\omega^2)}$  is the typical size of the condensate,  $\xi_h = \hbar/\sqrt{m\mu}$  is the healing length with  $\mu = g\rho(0)$ , and we used  $\zeta^{-1} = 25$ ,  $\zeta^{-1} = 50$  and  $\zeta^{-1} = 100$ , corresponding to  $(N, \langle \delta \hat{N} \rangle) = (121, 34)$ ,  $(N, \langle \delta \hat{N} \rangle) = (489, 145)$  and  $(N, \langle \delta \hat{N} \rangle) = (1962, 608)$  respectively. The homogeneous momentum distribution, Eq. (17), is also plotted for comparison, yielding good agreement with the common envelope function traced out by  $\langle \delta \hat{n}_{\mathbf{k}} \rangle^2 / R_c^2$  as  $\omega$  decreases. Inset: non-condensed contribution  $\langle \delta \hat{n}_{\mathbf{k}} \rangle^2 / R_c^2$ , plotted as a function of  $k R_c$  for  $\tilde{g} = 4$  and  $\zeta^{-1} = 25$ , using logarithmic scale on both axis. Homogeneous distribution, Eq. (17), is also shown. For large wave numbers  $|\mathbf{k}| \gg 1/\xi_h$ , the universal power law decay  $\sim 1/|\mathbf{k}|^4$  is recovered.

symmetric system. To make a quantitative comparison with our numerical results, plotted in Fig. 5, to Eq. (17), we have chosen  $\rho_0$  as the average density of the inhomogeneous trapped gas. In the limit of small confining frequency  $\omega$ , the condensate is well described by the Thomas-Fermi profile, yielding  $\rho_0 = \rho(0)/2$ .

We find good agreement with the common envelope function without any further fitting parameter. The non-condensed contribution,  $\langle \delta \hat{n}_{\mathbf{k}} \rangle$ , decays as  $\sim 1/|\mathbf{k}|$  for wave numbers  $1/R_c \ll |\mathbf{k}| \ll 1/\xi_h$ , while for even larger momenta,  $|\mathbf{k}| \gg 1/\xi_h$ , the expected  $\sim 1/|\mathbf{k}|^4$  decay is recovered (see inset of Fig. 5) [30, 49, 50].

### C. Correlation functions

In Section II A, we derived the correlation function  $C(\mathbf{k}, \mathbf{k}') = \langle \delta \hat{n}_{\mathbf{k}} \delta \hat{n}_{\mathbf{k}'} \rangle$  within the particle number conserving Bogoliubov approach, and separated the leading ( $\sim |\delta\psi|^2$ ) and subleading ( $\sim |\delta\psi|^4$ ) contributions from the leading shot noise signal in the terms  $C^{(1)}(\mathbf{k}, \mathbf{k}')$  and  $C^{(2)}(\mathbf{k}, \mathbf{k}')$ , respectively. These contributions, given by Eqs. (14a) and (14b), are plotted in Fig. 6 for wave numbers  $\mathbf{k}' = \mathbf{k}$  and  $\mathbf{k}' = -\mathbf{k}$  for various interaction

strengths  $\tilde{g}$ . The variance of the particle number  $\hat{n}(\mathbf{k})$  is given by the sum of the singular shot noise term and the diagonal correlations  $C(\mathbf{k}, \mathbf{k})$ , so the diagonal part  $C(\mathbf{k}, \mathbf{k})$  is not necessarily positive. However, the off-diagonal part  $C(\mathbf{k}, -\mathbf{k})$  develops a more pronounced anticorrelation dip, due to the depletion of the condensate by quasiparticle excitations.

The non-connected part  $\langle \hat{n}_{\mathbf{k}} \rangle \langle \hat{n}_{\mathbf{k}'} \rangle$  of the correlator  $\langle \hat{n}_{\mathbf{k}} \hat{n}_{\mathbf{k}'} \rangle$  does not distinguish between diagonal and off-diagonal correlations, and follows readily from Fig. 4. Although this large signal is subtracted in the correlation function, Eq. (13), it still provides a large background in an experiment and may therefore be hard to separate it from the more interesting part of the signal (see Fig. 7). Similar to  $\langle \hat{n}_{\mathbf{k}} \rangle$ , the product  $\langle \hat{n}_{\mathbf{k}} \rangle \langle \hat{n}_{\mathbf{k}'} \rangle$  exhibits a sharp peak with typical width  $|\mathbf{k}'| \sim |\mathbf{k}| \sim 1/R_c$ , originating from the single-mode condensate, also shown in Fig. 4. The expectation values  $\langle \hat{n}_{\mathbf{k}} \rangle$  being invariant under rotations,  $\langle \hat{n}_{\mathbf{k}} \rangle \langle \hat{n}_{\mathbf{k}'} \rangle$  is clearly also independent of the relative directions of  $\mathbf{k}$  and  $\mathbf{k}'$ , and is 'cylindrically' symmetrical.

The leading contribution  $C^{(1)}$ , shown in the top panels of Fig. 6, accounts for correlations between the single-mode condensate and the non-condensed fraction of the gas. Consequently, similar to  $\varphi_0(\mathbf{k})$ ,  $C^{(1)}$  is constrained to small wave numbers, and decreases rapidly for  $|\mathbf{k}| > 1/R_c$ . The function  $C^{(1)}$  exhibits an *anticorrelation dip* in the off-diagonal  $\mathbf{k}' \approx -\mathbf{k}$  for wave numbers  $|\mathbf{k}| \sim 1/R_c$ . This dip dominates the small momentum behavior of  $C(\mathbf{k}, \mathbf{k}')$ , and gets more pronounced for increasing interaction strength. The negative correlation observed originates from particle number preserving processes, where the interaction  $g$  creates quasiparticle pairs from the condensate. The coherent transfer of these particle pairs between the single-mode condensate and the non-condensed fraction of gas is responsible for the anticorrelation dip in  $C^{(1)}$  (see also Section III D) [52]. Notice that this anticorrelation also appears in the standard grand canonical Bogoliubov approach: there the factors  $\varphi_0(\mathbf{k})$  and  $\varphi_0(\mathbf{k}')$  in the first four terms of Eq. (14a) emerge as the coherence factors of the condensate, and  $\varphi_0$  and  $\varphi_0^*$  correspond to removing or adding a particle to the condensate. Therefore, these terms can be associated with particle number conserving processes, captured to a certain degree already by the usual (non-conserving) Bogoliubov approach.

Finally, the contribution  $C^{(2)}$ , shown in the bottom panels of Fig. 6, describes correlations within the non-condensed (more precisely, non single-mode condensed) cloud, but also incorporates contributions arising within the particle number conserving Bogoliubov approach, generated by the term  $-|\varphi_0(\mathbf{k})|^2 \delta \hat{N}$  in the expression of  $n_{\mathbf{k}}$ , Eq. (11). These latter contributions give rise to a central peak of width  $\sim 1/R_c$ , and yield a small correction to the leading order correlations between the single-mode condensate and the non-condensed particles, contained in  $C^{(1)}$ . Correlations within the non-condensed fraction, captured by the other terms in  $C^{(2)}$ , result in a *slowly decaying positive correlation tail* both in the di-

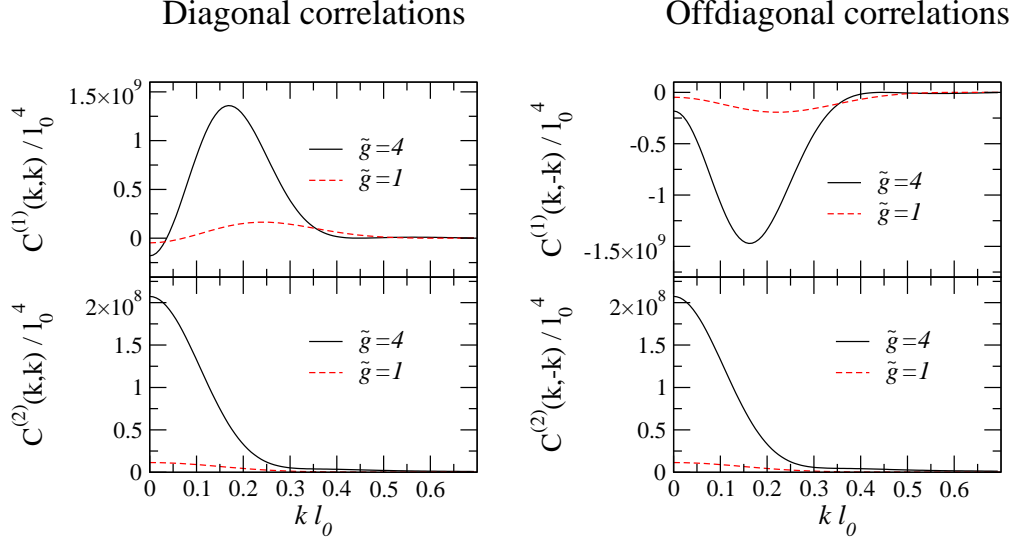


FIG. 6. Different contributions to dimensionless diagonal and offdiagonal correlation functions  $C(\mathbf{k}, \mathbf{k})/l_0^4$  and  $C(\mathbf{k}, -\mathbf{k})/l_0^4$ , plotted as a function of dimensionless wave number  $|\mathbf{k}|l_0$  for fixed  $N = 1962$  and for two different interaction strength  $\tilde{g} = 1$  and  $\tilde{g} = 4$ . Here  $l_0 = \sqrt{\hbar/(m\omega)}$  is the oscillator length, and the interaction values correspond to  $\langle \delta \hat{N} \rangle = 138$  and  $\langle \delta \hat{N} \rangle = 608$  respectively. The condensate-quasiparticle contribution  $C^{(1)}$  gives a positive peak in diagonal correlations, but gets negative in the offdiagonal, expressing that quantum fluctuations deplete the condensate. As in a homogeneous system, the quasiparticle-quasiparticle correlation  $C^{(2)}$  is positive both in the diagonal and in the offdiagonal. However, this contribution is much smaller than  $C^{(1)}$  for wave numbers of the order of  $1/R_c$ . The amplitude of the correlations  $C^{(1)}$  and  $C^{(2)}$  increases with increasing interaction strength, as the hybridization of the condensate with virtual excitations gets more pronounced.

agonal,  $\mathbf{k}' = \mathbf{k}$ , and in the offdiagonal,  $\mathbf{k}' = -\mathbf{k}$ . This positive correlation is qualitatively similar to the simple Bogoliubov result, valid for weakly interacting homogeneous condensates [32]. Albeit their contribution is small compared to the amplitude of the central peaks in  $C^{(1)}$ , quantum fluctuations dominate the correlation function for wave numbers  $|\mathbf{k}| \gg 1/R_c$ , showing that the fluctuating part of the ground state consists of *pairs* of quasiparticles, as visualized in Fig. 1. The amplitude of this correlation tail is sensitive to interactions, and is further enhanced by increasing interaction strength  $\tilde{g}$ .

To gain further insight into the structure of  $C(\mathbf{k}, \mathbf{k}')$ , we have plotted in Fig. 8 the correlation functions  $C^{(1)}(\mathbf{k}, \mathbf{k}')$  and  $C^{(2)}(\mathbf{k}, \mathbf{k}')$ , as functions of  $\mathbf{k}$  while keeping  $\mathbf{k}'$  fixed. For  $|\mathbf{k}'|$  of the order of  $1/R_c$ , opposite to the positive peak at  $\mathbf{k} = \mathbf{k}'$ , an anticorrelation dip arises around the wave number  $\mathbf{k} = -\mathbf{k}'$  in the condensate-quasiparticle contribution  $C^{(1)}$ , in accordance with the results plotted in Fig. 6. This structure, reflecting correlations between the quasiparticles and the condensate, disappears for wave numbers  $|\mathbf{k}'| \gg 1/R_c$  (bottom row in Fig. 8), where positive correlations appear for wave numbers  $\mathbf{k}$  opposite to  $\mathbf{k}'$ .

As shown in the bottom row of Fig. 8, for  $|\mathbf{k}'| \gg 1/R_c$  two narrow positive peaks can be observed in  $C^{(2)}$  around wave numbers  $\mathbf{k} = \mathbf{k}'$  and  $\mathbf{k} = -\mathbf{k}'$ . These positive contributions originate from pair correlations inside the non-condensed fraction of the gas, and are related to the slowly decaying positive tail of the diagonal and off-

diagonal correlation function, plotted in Fig. 6. These pair correlations dominate the tails of ToF images of the condensate. For small momenta,  $|\mathbf{k}'| \sim 1/R_c$ , however, the correlation function  $C^{(2)}$  is dominated by a central peak of typical width  $\sim 1/R_c$ , originating from subleading, fourth order corrections in the fluctuations  $\delta\psi$ .

#### D. Simple model for correlations

The structure of the correlation function  $C(\mathbf{k}, \mathbf{k}')$ , discussed above, provides detailed information on the ground state of the system. The slowly decaying positive tail around  $\mathbf{k} = -\mathbf{k}'$  for  $|\mathbf{k}| \gg 1/R_c$  is a sign of excitations created in pairs  $\mathbf{k}$  and  $-\mathbf{k}$ , characteristic to the familiar two-mode squeezed structure of the Bogoliubov wave function. On the other hand, the negative off-diagonal correlations found for  $|\mathbf{k}| \ll 1/R_c$  show that these pairs of excitations are created coherently from the single mode condensate by quantum fluctuations.

To illustrate the latter point, let us consider the correlations present in two different simple model states, both showing a pair structure of excitations. We first consider a pure state with coherently created excitations, then we calculate the correlations for a mixed state as well, where this coherence is lost. We show that a *p*-wave like structure of the correlation function only emerges in the first case, for coherent quantum fluctuations.

Let us first take the following pure state, with excita-

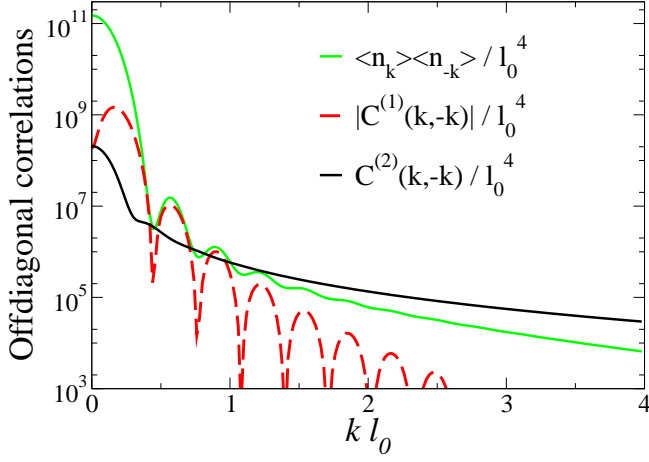


FIG. 7. Different contributions to dimensionless offdiagonal correlation function  $C(\mathbf{k}, -\mathbf{k})/l_0^4$ , plotted as a function of dimensionless wave number  $|\mathbf{k}|l_0$  for particle number  $N = 1962$  and interaction strength  $\tilde{g} = 4$ , using logarithmic scale on vertical axis. Here  $l_0 = \sqrt{\hbar/(m\omega)}$  is the oscillator length, and the interaction corresponds to  $\langle \delta \hat{N} \rangle = 608$ . The background signal  $\langle \hat{n}_{\mathbf{k}} \rangle \langle \hat{n}_{-\mathbf{k}} \rangle / l_0^4$  shows a steep decrease due to the disappearance of condensate wave function, followed by a slower decay as an effect of non-condensed particles. The condensate-quasiparticle contribution  $C^{(1)}$  is constrained to the regime of the single-mode condensate, and converges to zero rapidly for  $|\mathbf{k}| \gg 1/R_c$ . The quasiparticle-quasiparticle correlation  $C^{(2)}$  gives a slowly decaying tail, dominating the correlation function for  $|\mathbf{k}| \gg 1/R_c$ .

tions created in pairs,

$$|A\rangle = \left[ \left( \hat{b}_0^\dagger \right)^2 - g \hat{b}_+^\dagger \hat{b}_-^\dagger \right] |0\rangle.$$

Here  $\hat{b}_0^\dagger$  denotes a bosonic creation operator, corresponding to the condensate with the cylindrically symmetric wave function  $\varphi_0(\mathbf{r}) \equiv \varphi_s(r)$ . Similarly,  $\hat{b}_\pm^\dagger$  represent bosonic fluctuations ( $\delta\psi$ ), orthogonal to  $\varphi_0$ . By orthogonality they must have a  $p$ -wave structure in the simplest case:  $\varphi_\pm(\mathbf{r}) \equiv \varphi_p(r)e^{\pm i\varphi}$ , with  $(r, \varphi)$  denoting polar coordinates. Indeed, we verified numerically that the excitations with  $p$ -wave structure,  $s = (n, m = \pm 1)$ , give rise to the dominant contribution to  $C^{(1)}$ .

For a small admixture of the  $\varphi_\pm$  states,  $g \ll 1$ , the state  $|A\rangle$  can be used as a simple model capturing the  $\pm\mathbf{k}$  pair structure of the Bogoliubov ground state, with fixed particle number 2. Let us now calculate the correlations induced by  $|A\rangle$ ,  $C_A(\mathbf{k}, \mathbf{k}') = \langle A | \hat{\psi}^\dagger(\mathbf{k}) \hat{\psi}^\dagger(\mathbf{k}') \hat{\psi}(\mathbf{k}) \hat{\psi}(\mathbf{k}') | A \rangle$ , and inspect the different contributions ordered according to the power of  $g$ .

Using cylindrical coordinates  $\mathbf{k} \leftrightarrow (k, \theta)$ , we can express the Fourier transforms of the wave functions  $\varphi_{s,\pm}$

as

$$\varphi_s(\mathbf{k}) \equiv \varphi_s(k) = 2\pi \int dr r \varphi_s(r) J_0(kr),$$

$$\varphi_\pm(\mathbf{k}) \equiv -i \varphi_p(k) e^{\pm i\theta} = -i 2\pi \int dr r \varphi_p(r) J_1(kr) e^{\pm i\theta},$$

with  $J_0$  and  $J_1$  denoting Bessel functions. By using these relations, it is easy to see that the  $\sim g^0$  contribution to  $C_A(\mathbf{k}, \mathbf{k}')$  will be cylindrically symmetric. However, the terms proportional to  $g$  will give a contribution

$$\sim g \varphi_s(k) \varphi_s(k') \varphi_p(k) \varphi_p(k') \cos(\theta - \theta'). \quad (18)$$

This term has the same  $p$ -wave symmetry, as the condensate-quasiparticle correlation function  $C^{(1)}$ , and corresponds to positive correlations for  $\mathbf{k} = \mathbf{k}'$ , but results in an anticorrelation dip for  $\mathbf{k} = -\mathbf{k}'$ .

The terms proportional to  $g^2$  can be divided into a cylindrically symmetric contribution, and an additional term

$$\sim g^2 \varphi_p(k)^2 \varphi_p(k')^2 \cos(2(\theta - \theta')). \quad (19)$$

As expected from the pair structure built into  $|A\rangle$ , the  $d$ -wave symmetry of this contribution is consistent with the large wave number behavior of the quasiparticle-quasiparticle correlation function  $C^{(2)}$ , resulting in positive correlation for  $\mathbf{k} = \pm\mathbf{k}'$ . At the tails of the ToF image, however, all higher harmonics contribute to the density profile. Repeating the preceding analysis with  $\varphi_\pm(\mathbf{r}) \equiv \varphi_m(r)e^{\pm im\varphi}$  for arbitrary  $m$  shows that the term proportional to  $g^2$  depends on the angles  $\theta$  and  $\theta'$  as  $\cos(2m(\theta - \theta'))$ , still leading to positive correlations for  $\theta - \theta' \approx \pi$ . To contrast this even structure of  $C^{(2)}$  to the odd  $p$ -wave symmetry of  $C^{(1)}$ , we refer to it as a “ $d$ -wave” structure – in spite of the presence of higher harmonics.

In order to show, that the contribution given by Eq. (18) can indeed be identified as a sign of coherent quantum fluctuations, let us now consider a mixed state, exhibiting a pair structure similar to  $|A\rangle$ , described by the density matrix

$$\hat{\rho} = |B\rangle\langle B| + g^2 |C\rangle\langle C|,$$

with  $|B\rangle = (b_0^\dagger)^2 |0\rangle$  and  $|C\rangle = b_+^\dagger b_-^\dagger |0\rangle$ . The calculation of the correlation function  $\text{Tr} \left( \hat{\rho} \hat{\psi}^\dagger(\mathbf{k}) \hat{\psi}^\dagger(\mathbf{k}') \hat{\psi}(\mathbf{k}) \hat{\psi}(\mathbf{k}') \right)$  shows, that the first order contribution Eq. (18) disappears, while the quasiparticle-quasiparticle term, given by Eq. (19), persists. Thus the relative phase between the two terms in  $|A\rangle$ , i.e. the coherence of the interaction induced quasiparticle pairs, is crucial for the anticorrelations observed here and in Ref. [31].

#### IV. CONCLUSION

We have studied the momentum distribution and the density correlation function of a two-dimensional, harmonically trapped interacting Bose gas. Concentrating

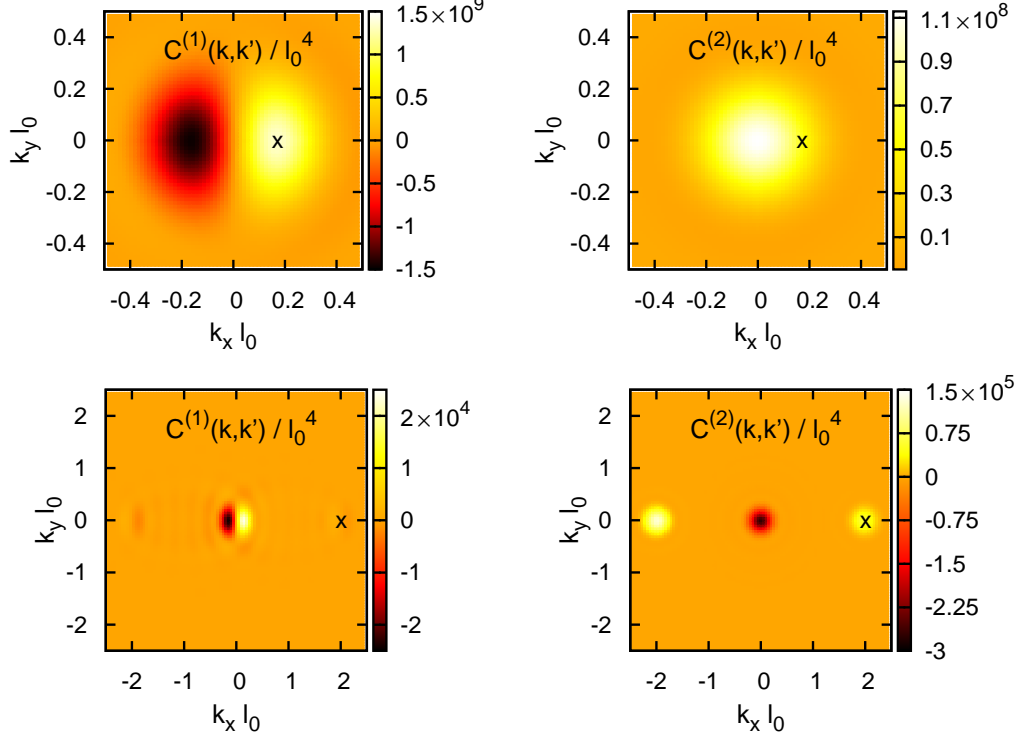


FIG. 8. Dimensionless correlation functions  $C^{(1)}(\mathbf{k}, \mathbf{k}')/l_0^4$  and  $C^{(2)}(\mathbf{k}, \mathbf{k}')/l_0^4$  plotted as a function of dimensionless wave number  $\mathbf{k}l_0$ , for fixed values of  $\mathbf{k}'$ . Here  $l_0 = \sqrt{\hbar/(m\omega)}$  oscillator length, and we have used  $\zeta^{-1} = 100$  and  $\tilde{g} = 4$ , corresponding to  $N = 1962$  particles and  $\langle \delta \hat{N} \rangle = 608$ . First row:  $\mathbf{k}'l_0 = (0.16, 0)$ . The condensate-quasiparticle correlation  $C^{(1)}$  is positive if  $\mathbf{k}$  and  $\mathbf{k}'$  point to the same direction, and gives negative contribution in the  $\mathbf{k}' \approx -\mathbf{k}$  regime. The positive correlation  $C^{(2)}$  is concentrated to small  $\mathbf{k}l_0$  wave numbers, due to subleading corrections to condensate-quasiparticle correlations contained in  $C^{(1)}$ . Second row:  $\mathbf{k}'l_0 = (2, 0)$ . The dominant contribution here is the quasiparticle-quasiparticle correlation  $C^{(2)}$ , giving negative values for small wave numbers, and narrow positive peaks around  $\mathbf{k} = \mathbf{k}'$  and  $\mathbf{k} = -\mathbf{k}'$ , expressing correlations in the non-condensed fraction of the gas.

on the interplay of quantum fluctuations, confinement and particle number conservation, we performed the calculations at zero temperature, using a particle number preserving Bogoliubov-approach.

To characterize the system, we have first calculated the momentum distribution function for various interaction strengths  $\tilde{g}$ , which is dominated by a central peak originating from the single-mode condensate. The amplitude of the non single-mode condensed fraction of the gas is clearly overwhelmed by this central peak. However, this latter contribution is much more extended in Fourier space, giving a slowly decaying tail. Therefore, it can possibly be disentangled from the single-mode condensate peak experimentally.

By studying the correlation function  $C(\mathbf{k}, \mathbf{k}') \equiv \langle \delta \hat{n}_{\mathbf{k}} \delta \hat{n}_{\mathbf{k}'} \rangle$ , we showed that the *anti-correlations* between opposite wave numbers  $\mathbf{k}$  and  $-\mathbf{k}$ , experimentally observed for one-dimensional quasi-condensates [31], also appear for higher,  $d = 2$  dimensional systems. Moreover, by separating  $C(\mathbf{k}, \mathbf{k}')$  into two parts, we identified two distinct contributions to the correlation function, exhibiting different symmetries.

The first contribution,  $C^{(1)}$ , describing correlations between the single-mode condensate and the non-condensed fraction of the gas, is responsible for the development of the anti-correlation dip around  $\mathbf{k}' = -\mathbf{k}$ . This dip seems to originate from particle number preserving processes, coherently moving particle pairs between the single mode condensate and the non-condensed cloud. For our  $d = 2$  dimensional system at  $T = 0$  temperature, the spatial extension of the condensate,  $R_c$ , takes over the role of thermal wave length  $l_\phi$ , determining the region of anti-correlations in a one-dimensional quasi-condensate [31], thus the momentum-space extension of the anti-correlation dip is set by  $1/R_c$ .

In addition to the anticorrelations between nearly opposite wave numbers,  $\mathbf{k} \approx -\mathbf{k}'$ , mentioned above,  $C^{(1)}$  also contains *forward correlation* for particles of similar momenta,  $\mathbf{k} \approx \mathbf{k}'$ . The momentum space correlations between the single-mode condensate and the non-condensed fraction of the gas,  $C^{(1)}$ , thus exhibit a characteristic *p-wave* structure, and dominate the full correlation function  $C(\mathbf{k}, \mathbf{k}')$  in the region of small wave numbers  $|\mathbf{k}|, |\mathbf{k}'| \sim 1/R_c$ .

The other part of the correlation function,  $C^{(2)}$ , stems from correlations within the non-condensed fraction of the gas. It decays slowly as  $\sim 1/|\mathbf{k}|^2$  with a positive tail around the offdiagonal  $\mathbf{k}' \approx -\mathbf{k}$ , similarly to the Bogoliubov result for homogeneous systems. This contribution exhibits a "d-wave"-like symmetry with positive correlations both in the  $\mathbf{k}' \approx \mathbf{k}$  and  $\mathbf{k}' \approx -\mathbf{k}$  regimes, and dominates the full correlation function in the region of large wave numbers,  $|\mathbf{k}|, |\mathbf{k}'| \gg 1/R_c$ , where short distance correlations at scales  $\lambda \ll R_c$  are probed.

The anticorrelations observed seem to rely on several important ingredients: First, they reflect the dominant  $p$ -wave character of the quantum fluctuations, as supported by a careful analysis of the interaction-induced quantum fluctuations [53]. Second, they evidence the coherent nature of these quantum fluctuations. Finally, they appear to be related to processes, where particles move between the single mode part of the condensate and the fluctuating part,  $\delta\psi$ . Indeed, all important features discussed in the previous paragraphs can be captured by a simple toy model incorporating these three ingredients (see Section IIID). The contributions  $C^{(1)}$  and  $C^{(2)}$  reveal important information about the structure of the interacting superfluid state. The even symmetry of  $C^{(2)}$  reflects that long wave length excitations are created in pairs  $\pm\mathbf{k}$  from the single mode condensate, while the  $p$ -wave structure of  $C^{(1)}$  evidences the coherence of the quantum fluctuations.

In actual experiments, one measures the full correlator  $\langle \hat{n}_{\mathbf{k}} \hat{n}_{\mathbf{k}'} \rangle$  instead of the connected part  $C(\mathbf{k}, \mathbf{k}')$ , yielding a large, cylindrically symmetric background signal  $\langle \hat{n}_{\mathbf{k}} \rangle \langle \hat{n}_{\mathbf{k}'} \rangle$ . This results in a background  $\sim N^{1/2}$  times larger than the anti-correlation dip in the connected part around  $\pi/R_c$ . However,  $C^{(1)}$  exhibits a different,  $p$ -wave symmetry, making its experimental detection possible.

On the other hand, the positive "d-wave"-like tail of  $C(\mathbf{k}, \mathbf{k}')$  scales as  $\sim (N\tilde{g})^2$ . Being of the same order of magnitude as the background, it could be experimentally accessible. To observe these correlations, however, one needs to investigate the tails of the ToF image with momenta  $|\mathbf{k}| \gtrsim 1/R_c$ .

## ACKNOWLEDGMENTS

This research has been supported by the National Research, Development and Innovation Office - NKFIH Nos. K105149, SNN118028, K119442 and by the Bolyai Program of the Hungarian Academy of Sciences. ED acknowledges support from Harvard-MIT CUA, NSF Grant No. DMR-1308435, AFOSR Quantum Simulation MURI, AFOSR MURI Photonic Quantum Matter, the Humboldt Foundation, and the Max Planck Institute for Quantum Optics.

- 
- [1] R. Hanbury Brown and R. Q. Twiss, *Nature* **177**, 27 (1956).
  - [2] M. Yasuda and F. Shimizu, *Phys. Rev. Lett.* **77**, 3090 (1996).
  - [3] H. Kiesel, A. Renz and F. Hasselbach, *Nature* **418**, 392 (2002).
  - [4] G. D. Mahan, *Many Particle Physics* (Plenum, New York, 1981).
  - [5] N. W. Ashcroft and N. D. Mermin, *Solid State Physics* (Saunders, Philadelphia, 1976).
  - [6] E. Altman, E. Demler and M. D. Lukin, *Phys. Rev. A* **70**, 013603 (2004).
  - [7] S. Fölling, F. Gerbier, A. Widera, O. Mandel, T. Gericke and I. Bloch, *Nature* **434**, 481 (2005).
  - [8] M. Schellekens, R. Hoppeler, A. Perrin, J. Viana Gomes, D. Boiron, A. Aspect and C. I. Westbrook, *Science* **310**, 648 (2005).
  - [9] C.-L. Hung, X. Zhang, N. Gemelke and C. Chin, *Nature* **470**, 236 (2011).
  - [10] N. Gemelke, X. Zhang, C.-L. Hung and C. Chin, *Nature* **460**, 995 (2009).
  - [11] T. Rom, Th. Best, D. van Oosten, U. Schneider, S. Fölling, B. Paredes and I. Bloch, *Nature* **444**, 733 (2006).
  - [12] M. Greiner, C. A. Regal, J. T. Stewart and D. S. Jin, *Phys. Rev. Lett.* **94**, 110401 (2005).
  - [13] V. Guarnera, N. Fabbri, L. Fallani, C. Fort, K. M. R. van der Stam and M. Inguscio, *Phys. Rev. Lett.* **100**, 250403 (2008).
  - [14] I. B. Spielman, W. D. Phillips and J. V. Porto, *Phys. Rev. Lett.* **98**, 080404 (2007).
  - [15] D. M. Weld and W. Ketterle, *Journal of Physics: Conference Series* **264**, 012017 (2011).
  - [16] J. Simon, W. S. Bakr, R. Ma, M. E. Tai, P. M. Preiss and M. Greiner, *Nature* **472**, 307 (2011).
  - [17] A. Perrin, R. Bcker, S. Manz, T. Betz, C. Koller, T. Plisson, T. Schumm and J. Schmiedmayer, *Nat. Phys.* **8**, 195 (2012).
  - [18] P. Törmä and K. Sengstock, *Quantum Gas Experiments: Exploring Many-Body States* (Imperial College Press, 2014).
  - [19] Z. Hadzibabic, S. Stock, B. Battelier, V. Bretin and J. Dalibard, *Phys. Rev. Lett.* **93**, 180403 (2004).
  - [20] M. Greiner, O. Mandel, T. Esslinger, T. W. Hänsch and I. Bloch, *Nature* **415**, 39 (2002).
  - [21] A. Görlitz, J. M. Vogels, A. E. Leanhardt, C. Raman, T. L. Gustavson, J. R. Abo-Shaeer, A. P. Chikkatur, S. Gupta, S. Inouye, T. Rosenband and W. Ketterle, *Phys. Rev. Lett.* **87**, 130402 (2001).
  - [22] W. S. Bakr, J. I. Gillen, A. Peng, S. Fölling and M. Greiner, *Nature* **462**, 74 (2009).
  - [23] T. Schumm, S. Hofferberth, L. M. Andersson, S. Wildermuth, S. Groth, I. Bar-Joseph, J. Schmiedmayer and P. Krüger, *Nat. Phys.* **1**, 57 (2005).
  - [24] Z. Hadzibabic, P. Krüger, M. Cheneau, B. Battelier and J. Dalibard, *Nature* **441**, 1118 (2006).
  - [25] Low dimensional systems are realized in highly anisotropic traps. When the confinement is removed, the interactions quickly become negligible due to the rapid

- expansion of the gas in the tightly confined directions.
- [26] A. L. Gaunt, T. F. Schmidutz, I. Gotlibovych, R. P. Smith and Z. Hadzibabic, Phys. Rev. Lett. **110**, 200406 (2013).
  - [27] S. P. Rath, T. Yefsah, K. J. Günter, M. Cheneau, R. Desbuquois, M. Holzmann, W. Krauth and J. Dalibard, Phys. Rev. A **82**, 013609 (2010).
  - [28] L. Chomaz, L. Corman, T. Bienaim, R. Desbuquois, C. Weitenberg, S. Nascimbene, J. Beugnon and J. Dalibard, Nat. Comm. **6**, 6172 (2015).
  - [29] P. Krüger, Z. Hadzibabic, J. Dalibard, Phys. Rev. Lett. **99**, 040402 (2007).
  - [30] R. Chang, Q. Bouton, H. Cayla, C. Qu, A. Aspect, C. I. Westbrook and D. Clément, arXiv:1608.04693.
  - [31] B. Fang, A. Johnson, T. Roscilde, and I. Bouchoule, Phys. Rev. Lett. **116**, 050402 (2016).
  - [32] L. Mathey, A. Vishwanath and E. Altman, Phys. Rev. A **79**, 013609 (2009).
  - [33] T. M. Wright, A. Perrin, A. Bray, J. Schmiedmayer and K. V. Kheruntsyan, Phys. Rev. A **86**, 023618 (2012).
  - [34] A. Imambekov, I. E. Mazets, D. S. Petrov, V. Gritsev, S. Manz, S. Hofferberth, T. Schumm, E. Demler and J. Schmiedmayer, Phys. Rev. A **80**, 033604 (2009).
  - [35] I. Bouchoule, M. Arzamasovs, K. V. Kheruntsyan, D. M. Gangardt, Phys. Rev. A **86**, 033626 (2012).
  - [36] N. N. Bogoliubov, D. V. Shirkov, Introduction To the Theory of Quantized Fields (John Wiley & Sons, 1980).
  - [37] This limit is relevant for the regime  $\rho_{2D}\hbar^2/mk_BT \gg 1$ , where phase fluctuations are suppressed.
  - [38] Y. Castin and R. Dum, Phys. Rev. A **57**, 3008 (1998).
  - [39] In reality, the delta potential is not well defined, and a renormalization procedure must be employed. At the mean field level, considered here, however,  $g$  can be replaced by its renormalized value.
  - [40] I. Bloch, J. Dalibard and W. Zwerger, Rev. Mod. Phys. **80**, 885 (2008).
  - [41] Ch. Mora and Y. Castin, Phys. Rev. A **67**, 053615 (2003).
  - [42] D. S. Petrov, D. M. Gangardt, and G. V. Shlyapnikov, J. Phys. IV **116**, 5 (2004).
  - [43] J. Dziarmaga and K. Sacha, Phys. Rev. A **67**, 033608 (2003).
  - [44] M. Lewenstein and L. You, Phys. Rev. Lett. **77**, 3489 (1996).
  - [45] The last term in  $C^{(1)}$ ,  $-N|\varphi_0(\mathbf{k})|^2|\varphi_0(\mathbf{k}')|^2$ , originates from the completeness relation (9), and ensures that the variance of the total particle number remains zero,  $\langle \delta^2 \hat{N} \rangle = \int d^2\mathbf{k}/(2\pi)^2 \int d^2\mathbf{k}'/(2\pi)^2 C(\mathbf{k}, \mathbf{k}') = 0$ . A similar term also appears in the grand canonical description of the condensate, but eventually gets cancelled by the fluctuations in the total particle number, leading to  $\langle \delta^2 \hat{N} \rangle > 0$ .
  - [46] C. Gies and D. A. W. Hutchinson, Phys. Rev. A **70**, 043606 (2004).
  - [47] P. Öhberg, E. L. Surkov, I. Tittonen, S. Stenholm, M. Wilkens and G. V. Shlyapnikov, Phys. Rev. A **56**, R3346(R) (1997).
  - [48] In Eqs. (12) and (13) a finite cutoff is introduced in the summation over  $s$ .
  - [49] S. Tan, Annals of Physics, **323**, 2952 (2008).
  - [50] L. Viverit, S. Giorgini, L. P. Pitaevskii, and S. Stringari, Phys. Rev. A **69**, 013607 (2004).
  - [51] Y. Castin, Bose-Einstein condensates in atomic gases: simple theoretical results. In R. Kaiser, C. Westbrook, and F. David, editors, *Coherent atomic matter waves, Lecture Notes of Les Houches Summer School*, EDP Sciences and Springer-Verlag, 2001.
  - [52] Interestingly, finite temperature calculations for trapped ideal bosons with a fixed total particle number revealed the presence of an anticorrelation peak in the offdiagonal correlation function [33].
  - [53] In one dimension, where these anticorrelations have been experimentally observed,  $s$ - and  $p$ -wave fluctuations correspond to fluctuations in the 'even' and 'odd' channels, respectively.